Upstream-generated Pc3 ULF wave signatures observed near the Earth's cusp

T. K. Yeoman,[1] D. M. Wright,[1] M. J. Engebretson,[2] M. R. Lessard,[3] V. A. Pilipenko,[2,4] and H. Kim[3,5]

Received 3 November 2011; revised 10 January 2012; accepted 18 January 2012; published 1 March 2012.

[1] Pc3 pulsations (frequency ~20–100 mHz) which originate in the ion foreshock upstream of the Earth's bow shock due to the interaction between reflected ions and the solar wind are frequently observed in ground-based pulsation magnetometer data. Previous studies have noted increased Pc3 wave power in the vicinity of the dayside cusp and inferred that the upstream waves gained entry via the cusp, although more recent studies have revealed a more complex picture. Here, we examine Pc3 wave power near local noon observed by search coil magnetometers at three closely-spaced stations on Svalbard, during times when an extended interval of HF radar backscatter indicative of the cusp is detected by the Hankasalmi SuperDARN radar. The location of the equatorward edge of the HF radar cusp may then be directly compared with the Pc3 wave power measured at three latitudes as the cusp migrates across the stations on a statistical basis. These observations are more consistent with wave entry to the magnetosphere along closed field lines equatorward of the cusp via the ionospheric transistor mechanism of Engebretson et al. (1991a), or weakly coupled fast and Alfvén wave modes, which then map to the low-latitude boundary layer or outer magnetosphere, rather than with wave entry into the magnetosphere via the cusp proper or exterior cusp.

Citation: Yeoman, T. K., D. M. Wright, M. J. Engebretson, M. R. Lessard, V. A. Pilipenko, and H. Kim (2012), Upstream-generated Pc3 ULF wave signatures observed near the Earth's cusp, *J. Geophys. Res.*, *117*, A03202, doi:10.1029/2011JA017327.

1. Introduction

[2] The influence of the Interplanetary Magnetic Field (IMF) on Ultra Low Frequency (ULF) waves in the Pc3 frequency band (frequency ~20–100 mHz) observed in the dayside magnetosphere has been known since *Troitskaya et al.* [1971] demonstrated that whenever the cone angle, θ_{xB}, of the IMF dropped below a certain threshold, enhanced ULF power was observed. This was explained by attributing the wave generation process to populations of backstreaming ions at the bow shock which are most likely to occur during times of low IMF cone angles. These backstreaming ions resonantly interact with naturally occurring waves in the solar wind, amplifying them [*Gary*, 1981]. As the propagation speed for ULF waves in the solar wind is significantly lower than the solar wind flow speed, these ULF waves are convected toward the Earth. In addition to cone angle control of the wave occurrence, the IMF magnitude also controls the peak frequency at which waves are generated. *Takahashi et al.* [1984] found that the peak frequency of waves observed inside the dayside magnetosphere, f, was dependent on both the IMF strength B and θ_{xB}. Observational evidence supporting this mechanism is reviewed by *Odera* [1986] and *Greenstadt et al.* [1981].

[3] Modeling studies by *Krauss-Varban* [1994] have suggested that the compressional waves generated upstream of the bow shock traverse the bow shock, magnetosheath and magnetopause without significant changes to their spectrum. However, observations suggest that narrowband wave activity is rarely observed within the magnetosheath, but rather broadband wave signatures of both a compressional and transverse nature [*Engebretson et al.*, 1991b; *Lin et al.*, 1991a, 1991b]. *Engebretson et al.* [2000] found no significant influence on the IMF clock angle in conjugate measurements of Pc3 wave power. They concluded from this that the Pc3 power generated upstream of the bow shock was convected through the magnetosheath as a spatial structure to the subsolar magnetopause, rather than propagating as a wave. Such wave activity may still gain access to the magnetosphere, and drive broadband or narrowband wave activity there, acting as a conduit between the upstream wave source and the magnetospheric response.

[1]Department of Physics and Astronomy, University of Leicester, Leicester, UK.
[2]Department of Physics, Augsburg College, Minneapolis, Minnesota, USA.
[3]Space Science Center, University of New Hampshire, Durham, New Hampshire, USA.
[4]Space Research Institute, Moscow, Russia.
[5]Now at Center for Space Science and Engineering Research, Virginia Polytechnic Institute and State University, Blacksburg, Virginia, USA.

0148-0227/12/2011JA017327

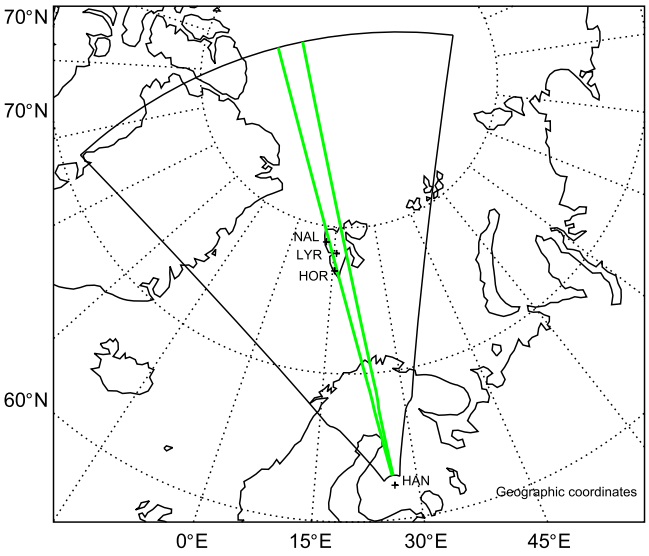

Figure 1. The field of view of the Hankasalmi, Finland SuperDARN radar. Channel A of the radar employed a full 16-beam scan, and is outlined in black. Channel B was restricted to beam 9, and is outlined in green. The locations of the three induction coil magnetometers on Svalbard (NAL, LYR, and HOR) are also marked.

[4] The exact mechanism through which Pc3 band power subsequently gains entry into the magnetosphere from the magnetosheath has received considerable attention, yet remains an open area of research. Early investigations from low latitudes suggested that the Pc3 wave power entered the magnetosphere via a wave coupling mechanism. At low latitudes Pc3 power may arise due to coupling to Field line Resonances (FLRs [*Southwood*, 1974]), where the resonant field line frequencies are appropriate for the Pc3 frequency range [*Yumoto et al.*, 1984, 1985]. At high latitudes, however, the fundamental resonant frequencies are lower, raising the question of how significant Pc3 power with an upstream origin reaches the high-latitude region where resonant field lines are not available.

[5] *Engebretson et al.* [1991a] investigated the distribution of AMPTE CCE (Active Magnetospheric Particle Tracer Explorers/Charge Composition Explorer) satellite measurements of Pc3 band power in magnetic local time and magnetic latitude, and also noted a similar modulation of the Pc3 pulsation power and precipitating magnetosheath/boundary layer electrons, proposing that the modulated electron fluxes provided an efficient conduit for wave power into the magnetosphere, via modulation of the ionospheric conductivity, in the so-called ionospheric transistor model. *Engebretson et al.* [1994a] used optical data to demonstrate that the particles involved were in fact trapped energetic particles (>5 keV) originating on closed outer magnetospheric field lines. In this model, as described subsequently by *Engebretson et al.* [2006], the peak wave power observed on the ground would map to outer magnetospheric field lines, reaching near the equatorward cusp boundary, but not within the cusp proper. The modulation of the ionospheric currents proposed in this model was demonstrated to result in large enough current systems to cause the observed magnetic perturbations by *Engebretson et al.* [1994b]. A number of subsequent studies [e.g., *Engebretson et al.*, 2000, and references therein] have argued that the spatial distribution of wave power on the ground is more consistent with such an entry mechanism, rather than one which involves a direct propagation of compressional wave power through the dayside magnetopause, and a subsequent propagation of this wave power throughout the magnetosphere with coupling to field-guided Alfvén modes. *Matsuoka et al.* [2002] used Geotail spacecraft data and data from ground magnetometers and coherent radars to suggest a close relationship between the Pc3 wave power and the cusp location, consistent with the ideas of *Engebretson et al.* [2000] although they also invoked the model of *Pilipenko et al.* [1999], which suggests a waveguide in the exterior cusp in order to explain the latitudinal profile of the wave power.

[6] By contrast, *Howard and Menk* [2005] more recently provided a detailed spectral analysis of a subset of Pc3-4 wave events which had a large spatial coherence length, observed in ground magnetometer array data. While *Howard and Menk* [2005] concluded that their maximum amplitude was close to the projected footprint of a modeled magnetopause, broadly consistent with the studies above, their interpretation was that fast mode waves entering the magnetosphere near the subsolar point were coupled to field-guided Alfvén modes, which could subsequently form standing oscillations more in line with the suggestions of *Yumoto et al.* [1984, 1985]. *Howard and Menk* [2005] considered a number of candidate mechanisms. A direct propagation of the fast mode from the subsolar point to the high latitude regions is one candidate. A fast mode which couples to field-guided modes in the outer magnetosphere might also drive those field lines to resonance at higher harmonics, although *Pilipenko and Engebretson* [2002] considered this to be unlikely. Coupling of the upstream wave source to cavity modes [e.g., *Kivelson et al.*, 1984] might also provide increased high latitude powers. *Howard and Menk* [2005] concluded that a direct propagation of the fast mode would not provide the observed high latitude peak, and found no evidence of the node/antinode structure expected for a cavity mode. They found some evidence of the driving of high latitude field line resonances at high harmonics for a minority of events, but concluded that wave entry at the subsolar point as a compressional wave, with subsequent weak coupling to field-guided Alfvén waves, was the most likely mechanism. Their study was, however, restricted to events with a large spatial coherence length, which may not be typical of the overall wave power in the Pc3 frequency band, nor did their events show any clear signs of the frequency dependence on the IMF magnitude expected for upstream-generated events [*Takahashi et al.*, 1984].

[7] The scenario of *Howard and Menk* [2005] is consistent with two recent case studies. *Clausen et al.* [2008] detected Pc3 wave power interpreted as having an upstream source over a wide range of ground locations and presented evidence for mode coupling to Alfvén waves within the magnetosphere. *Clausen et al.* [2009] observed the upstream Pc3 wave power directly in the solar wind. Field lines driven at their natural frequencies within the magnetosphere were simultaneously observed by the Cluster satellites, and wave power was also observed on the ground by magnetometers. In both these cases the evidence for mode coupling to Alfvén waves was noted fairly deep in the magnetosphere at $L \sim 5$.

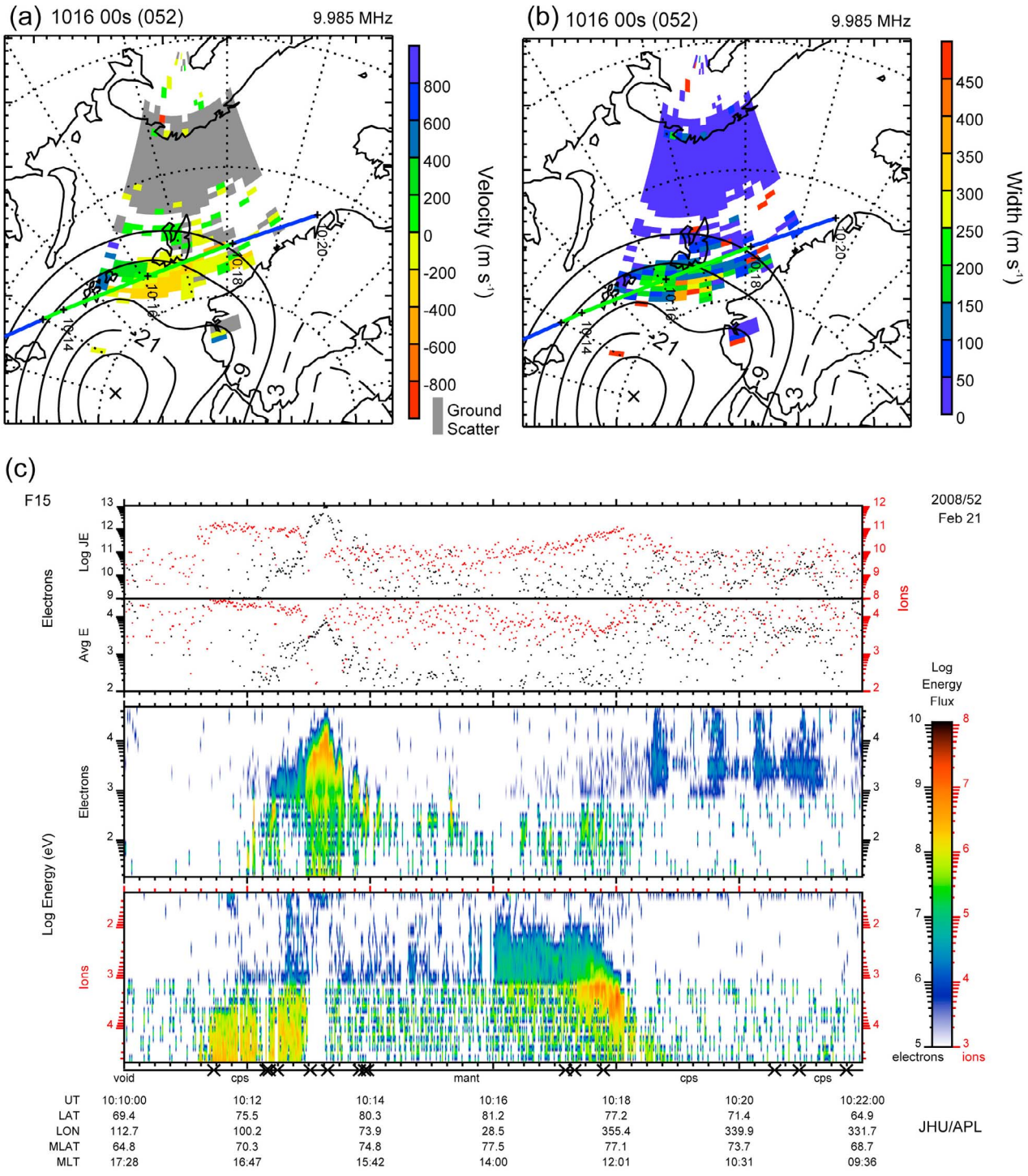

Figure 2. (a) Color-coded velocity data from Channel A of the Hankasalmi radar at 10:16 UT on February 21, 2008, in magnetic local time-magnetic latitude coordinates. Potential contours derived from velocity data from the full SuperDARN array are also illustrated. (b) Color-coded spectral width data in the same format as Figure 2a. (c) A DMSP spectrogram from 10:10 UT to 10:22 UT on February 21, 2008. The spacecraft track is shown in Figures 2a and 2b, where blue indicates regions of the track equatorward of the poleward boundary of energetic electron precipitation indicative of closed field lines, and green indicates regions poleward of this.

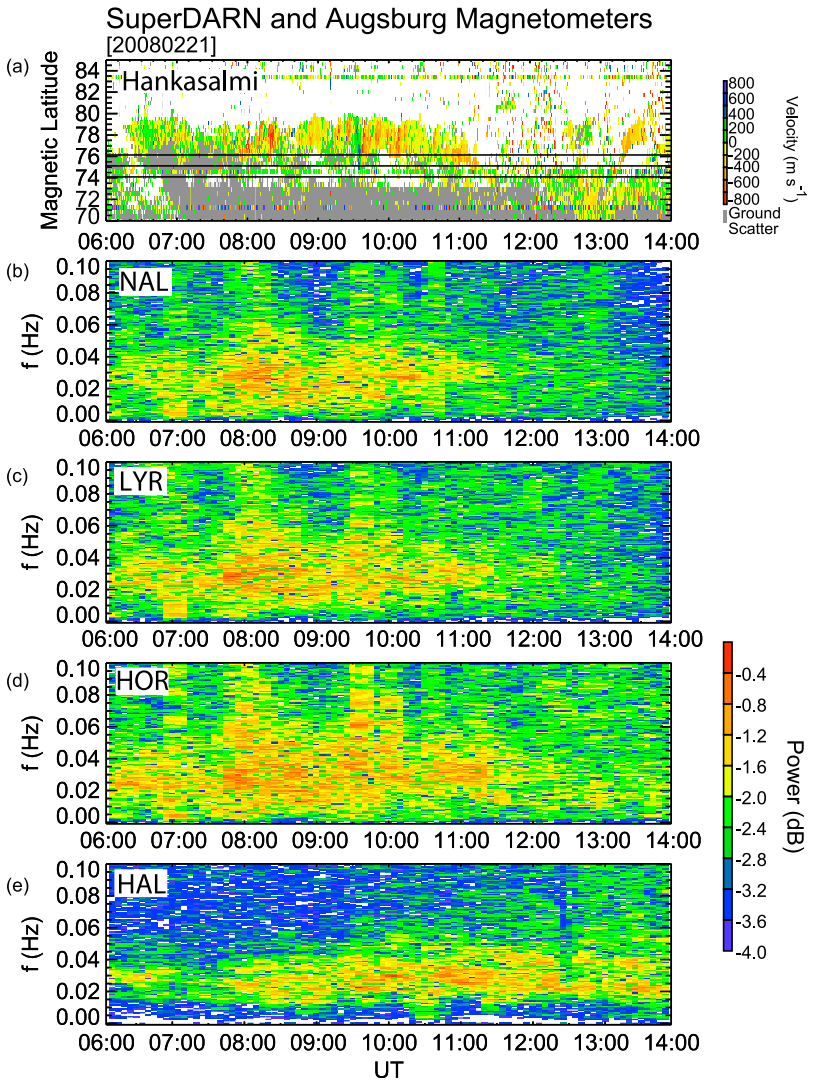

Figure 3. Radar and induction coil magnetometer data from 06:00 to 14:00 UT on February 21, 2008. (a) Color-coded velocity data from Channel B of the Hankasalmi radar as a function of magnetic latitude. The magnetic latitudes of the induction coil magnetometers at NAL, LYR and HOR are indicated with horizontal black lines. (b–d) Dynamic spectra of data from the 3 Svalbard induction coil magnetometers. (e) Dynamic spectrum of data from the antarctic Halley induction coil magnetometer.

[8] Here we approach the subject of the wave entry mechanism through a statistical comparison of the Pc3 wave power in the cusp region with direct observations of the location of the overlying cusp, provided through the spectral width boundary of HF coherent radar data, in order to investigate the validity of the various mechanisms proposed above.

2. Instrumentation

[9] The location of the cusp in this study was monitored by spectral width data [*Ponomarenko et al.*, 2007] from the SuperDARN radar at Hankasalmi, Finland. Full details of SuperDARN are given by *Greenwald et al.* [1995] and *Chisham et al.* [2007]. Figure 1 presents the field of view of the radar scan mode used in this study. Hankasalmi is a Stereo SuperDARN radar [*Lester et al.*, 2004], sounding two radar channels simultaneously. Here channel A of the radar employed a full 16-beam scan of 45 km range gates, starting at a range of 180 km, and is outlined in black. Channel B was restricted to a single beam, beam 9, pointing northward again with 45 km range gates. This beam is outlined in green in Figure 1. The integration time of the radar was 3 s, yielding a full radar scan from Channel A every minute, and single beam data with 3 s time resolution on Channel B. The range-finding algorithm used here includes the corrections for one and a half hop ionospheric backscatter as discussed by *Yeoman et al.* [2001], *Chisham et al.* [2008] and *Yeoman et al.* [2008].

[10] Data are also presented from three induction coil magnetometers (Ny Ålesund, NAL, 76.3° Corrected Geomagnetic (CGM) latitude; Longyearbyen, LYR, 75.3° CGM latitude and Hornsund, HOR, 74.2° CGM latitude, see Figure 1). These instruments, the Augsburg College–University of New Hampshire magnetometer array, were deployed in a closely spaced array on Svalbard during September 2006

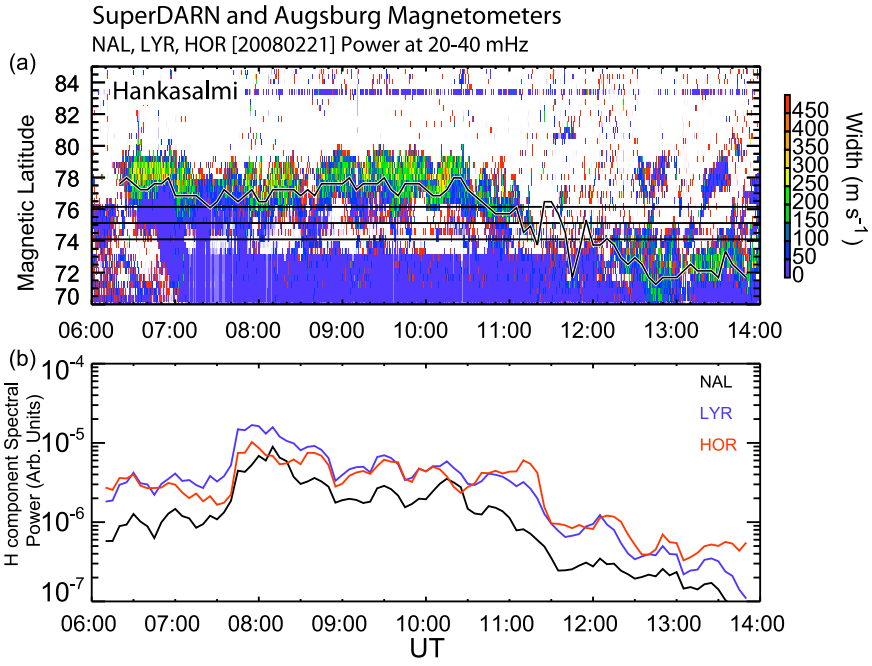

Figure 4. (a) Latitude-time-spectral width plot of data from beam 9 of the Hankasalmi SuperDARN radar from 06:00 to 14:00 UT on February 21, 2008. The magnetic latitudes of the induction coil magnetometers at NAL, LYR and HOR are indicated with horizontal black lines, and the spectral width boundary determined from the radar data, used here as a proxy for the cusp location, is indicated by a black curve (see text for details). (b) The time dependence of the spectral power in the 20–40 mHz frequency band derived from the induction coil magnetometers at NAL, LYR and HOR.

[*Engebretson et al.*, 2009]. These instruments are similar to those used for many years at several sites in Antarctica [*Engebretson et al.*, 2005], and data are also presented from the instrument there at Halley (HAL, −62° CGM latitude). Each instrument provides vector samples of dB/dt each 0.1 s in local geomagnetic coordinates with X northward and Y eastward. Here X component induction coil data is preprocessed by reducing the data to 0.5 s sampling, and then differencing the data in the time domain, as performed by *Engebretson et al.* [2000, 2005] to suppress low frequency wave activity, prior to the Fourier analysis described in section 3.

[11] Particle precipitation data are included from the SSJ/4 [*Hardy et al.*, 1984] instrument on DMSP F15. The DMSP satellites are in sun-synchronous polar orbits at an altitude of 840 km, and SSJ/4 points toward zenith, measuring ion and electron fluxes between 30 eV and 30 keV.

3. Data

[12] The data set investigated here was selected as follows. Intervals of significant Pc3 wave activity originating from upstream of the Earth's bow shock were initially selected by eye from spectrograms of induction coil magnetometer data from the three Svalbard magnetometer stations, during intervals when upstream data from the ACE spacecraft indicated that the IMF cone angle was conducive to upstream wave generation. The frequencies observed at Svalbard were consistent with those predicted from the upstream conditions, and the intervals chosen were restricted to intervals with a favorable cone angle. This yielded 30 days of data containing intervals for further examination from the ∼150 days of available 3–station data. Subsequently this list of events was reduced by applying the criteria that the SuperDARN Hankasalmi radar was running in the stereo mode described in section 2, where high time resolution were available on the Channel B beam overlying the magnetometer instruments, and that sufficient continuity of radar data was available at cusp latitudes to use the spectral width of the ionospheric backscatter as a proxy for the cusp position [*Baker et al.*, 1995; *Villain et al.*, 2002; *Chisham and Freeman*, 2003]. Application of these criteria produced 14 individual days for subsequent analysis, where the number of hours of useful data in a day varied from 2 to 8 hours in duration.

[13] A magnetic local time-magnetic latitude snapshot of line-of-sight (l-o-s) Doppler velocity and spectral width from the Hankasalmi SuperDARN radar at 10:16 UT during a typical day, February 21, 2008, is included in Figures 2a and 2b, respectively. Here magnetic latitude is marked by dotted circles, starting at 80°, magnetic local time is marked in 1-hour increments by radial dotted lines and local noon is at the top of the figure. In Figure 2a, antisunward velocities are observed in the noon high latitude ionosphere in the vicinity of the convection throat as identified by the global flow streamlines provided by the full SuperDARN array through the map potential technique [*Ruohoniemi and Greenwald*, 1996, 2005], and such observations are typical of HF radar data in the cusp region [e.g., *McWilliams et al.*, 2001]. Figure 2b reveals this area to be characterized by the high spectral widths typical of this region [*Baker et al.*, 1995]. Figure 2c presents a DMSP F15 spectrogram from 10:10 UT

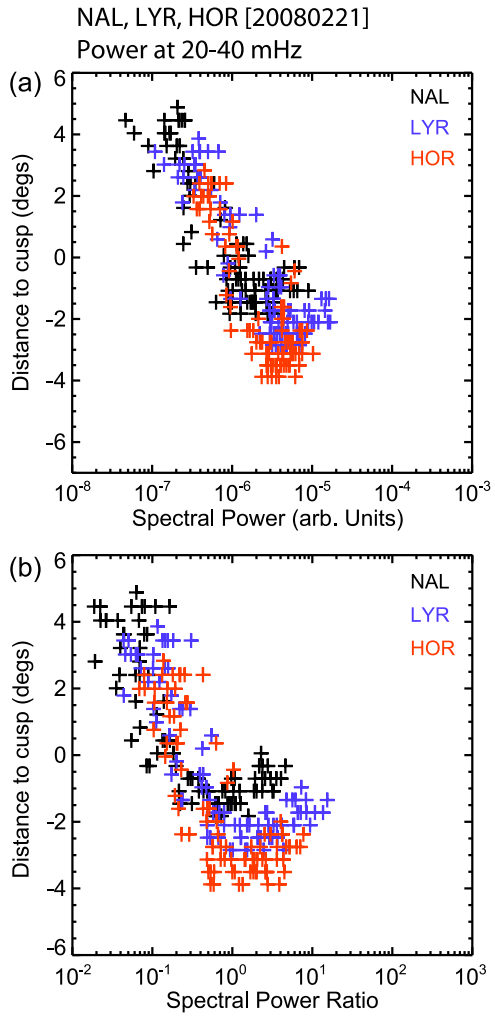

Figure 5. (a) A scatterplot of the NAL, LYR and HOR magnetometer spectral power as displayed in Figure 4b against the latitudinal separation of the magnetometer station from the spectral width cusp proxy indicated in Figure 4a. (b) As for Figure 5a but now plotting the magnetometer spectral power normalized by the concurrent spectral power measured by HAL.

to 10:22 UT. Two regions of energetic electron precipitation can be seen in the spectrogram, between 10:12:30–10:13:30 UT and 10:18:00–10:21:00 UT. Between these regions only low energy electrons, and some dispersed ion signatures are seen, as expected from the open field lines of the cusp and mantle regions [*Newell and Meng*, 1992]. The spacecraft track is shown in Figures 2a and 2b, where blue indicates regions of the track equatorward of the poleward boundary of the energetic electron precipitation indicative of closed field lines, and green indicates regions poleward of this. A good correspondence is seen between the latitudes bounded by the region of the satellite track colored green and the region of antisunward velocities and high spectral widths measured by the HF radar. Thus it can be demonstrated that the DMSP data provides an identification of the latitude of the cusp region which is consistent with that from the HF radars.

[14] Figure 3 presents the temporal development of the radar and magnetometer data between 06:00 UT and 14:00 UT on February 21, 2008. Figure 3a again presents the l-o-s Doppler velocity from the Hankasalmi SuperDARN radar, now as a function of time and magnetic latitude. Pulsed antisunward flows are observed throughout the interval, again typical of HF radar data in the cusp region [*McWilliams et al.*, 2001]. The location of the cusp scatter can be seen to evolve throughout the interval, being predominantly poleward of the locations of the three magnetometer stations (marked on the figure with horizontal lines) at the beginning of the interval, but migrating to equatorward of the magnetometers by the end of the interval. Figures 3b–3d present dynamic spectrograms of data from the three Svalbard magnetometers. In each case the 2 Hz sampled data from the magnetometers is subjected to an FFT analysis over a 20 min window, with a 5 min slip used in plotting the spectrograms. Significant spectral power is observed throughout most of the time interval under analysis, with the strongest powers being observed between 08:00 and 10:00 UT, centered between 20 and 40 mHz. The data from Halley, Antarctica in Figure 3e will be discussed later.

[15] The data are analyzed further in Figure 4. Figure 4a again shows a magnetic latitude-time plot of data from the Hankasalmi SuperDARN radar, but now spectral width is displayed. The HF radar spectral width boundary is routinely used as a proxy for the location of the cusp, as the data characteristically changes from low widths equatorward of the cusp on closed magnetic field lines to high spectral widths poleward of the cusp on open field lines [e.g., *Baker et al.*, 1995; *Villain et al.*, 2002; *Chisham and Freeman*, 2003]. Here we use a simple technique to locate this boundary between narrow and wide spectra, by determining the first latitude at which a spectrum with a width which exceeds 200 m s^{-1} is observed in the 3 s sampled Channel B data from Hankasalmi, and averaging this latitude over 5 min. The spectral width boundary determined by this technique is shown as a black line in Figure 4a, and can be visually seen to reasonably accurately follow the spectral width boundary, and thus allows a convenient automatic procedure for determining the latitudinal separation of the magnetometer stations (marked with horizontal black lines) from the cusp location. Figure 4b shows a time series of spectral power for each of the Svalbard magnetometer stations, derived from a summation of the spectral powers shown in Figure 3 between 20 and 40 mHz. Previously *Engebretson et al.* [2000] averaged wave power between 15–50 mHz, but the narrower band used here effectively covers the main wave activity in all the events under study. It can be seen that the spectral powers from the highest latitude station, NAL, are almost always lower than those at the lower latitudes. During the first half of the interval, when the cusp is at its highest latitudes, the spectral power at LYR is generally higher than that at the lowest station, HOR. In the second half of the interval, when the cusp moves equatorward, the power at HOR generally exceeds that at LYR, both when HOR is poleward and equatorward of the inferred cusp position.

[16] These dependencies of spectral power on the relative separations of the magnetometer stations and the cusp during this interval are explored further in Figure 5. Figure 5a presents a scatterplot of the spectral powers displayed in Figure 4b against the latitudinal separation of the magnetometer station and the cusp latitude proxy derived from

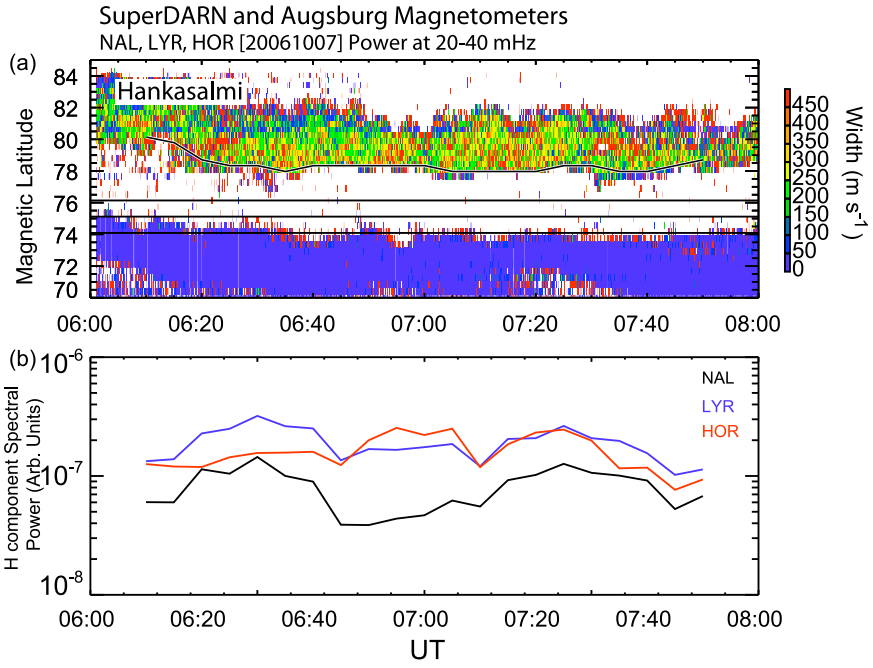

Figure 6. Radar and magnetometer data from 06:00 to 08:00 UT on October 27, 2006. The format is identical to that of Figure 4.

Figure 4a. Here positive values indicate magnetometer positions poleward of the cusp and negative values indicate magnetometer locations equatorward of the cusp. Data from each magnetometer station are color-coded as indicated in the figure legend. The spectral powers can be seen to be well ordered by the separation of the magnetometer station from the cusp, and from this interval the peak spectral power is recorded when the magnetometer stations are ~2° equatorward of the cusp latitude, although for this data interval coverage is limited for magnetometer–cusp separations further equatorward than this.

[17] Clearly any temporal variability of the wave power in the upstream wave generation region will also affect the wave power as registered on the ground magnetometers. In order to compensate for this variability, the wave power as measured far from the cusp region, at Halley, Antarctica, has also been measured, as shown in Figure 3e. These data, processed identically to the Svalbard magnetometer data, have been employed to normalize the Svalbard wave power for the effects of a variable upstream source, by computing the ratio of the wave power in the vicinity of the cusp, as measured at NAL, LYR, and HOR, to that as measured deeper in the magnetosphere at HAL. A scatterplot of this spectral power ratio is presented in Figure 5b. The spectral power ratio ranges from the cusp region power being an order of magnitude higher than the lower latitude power near the peak power region ~2° equatorward of the cusp, to the lower latitude power being almost 2 orders of magnitude greater than the cusp stations once those stations lie 4° poleward of the cusp location. For this interval the scatterplots of cusp region spectral power versus the distance to the cusp and spectral power ratio versus the distance to the cusp have a very similar form, implying that the variability of the upstream source was less important than the location of the magnetometer relative to the cusp in determining the measured spectral power in this case.

[18] A second interval of data from 06:00 UT to 08:00 UT on October 7, 2006 is presented in Figure 6, in the same format as Figure 4. In this case a shorter interval of continuous radar data are available, and as a result the cusp location is less variable. The wave power from NAL is again the weakest of the three Svalbard magnetometer stations. Wave power from LYR is highest at the beginning and the end of the interval, when the cusp latitude is highest, but wave power from the lowest latitude station at HOR dominates in the center of the interval, when the cusp latitude is at its lowest. A scatterplot of wave power (Figure 7a, in the same format as Figure 5a) shows less variability of wave power, as the range of latitude separations is more limited, but suggests a peak wave power in this case in the region ~3–4° equatorward of cusp. In Figure 7b the spectral power ratios show a similar clustering to the spectral powers, with in this case similar powers being observed near to the cusp and deeper in the magnetosphere at HAL.

[19] In Figure 8 the data from the full set of 14 days observations are combined together in a similar format to Figures 5a and 7a, providing a total of 1364 data points for comparison. In Figure 8a the data from each day of observation are color-coded in order to highlight the variability within and between the days of observation. These observations were taken in September and October 2006 and February and March 2008. Over the 14 days of observations, a range of separations from the magnetometer locations to the cusp location of between ~5° latitude equatorward and ~5° latitude poleward of the cusp were recorded. During the 14 days the variability of the cusp–magnetometer latitude separation in each individual day was between 2° and 8° latitude. Five of the 14 days showed a range of cusp–

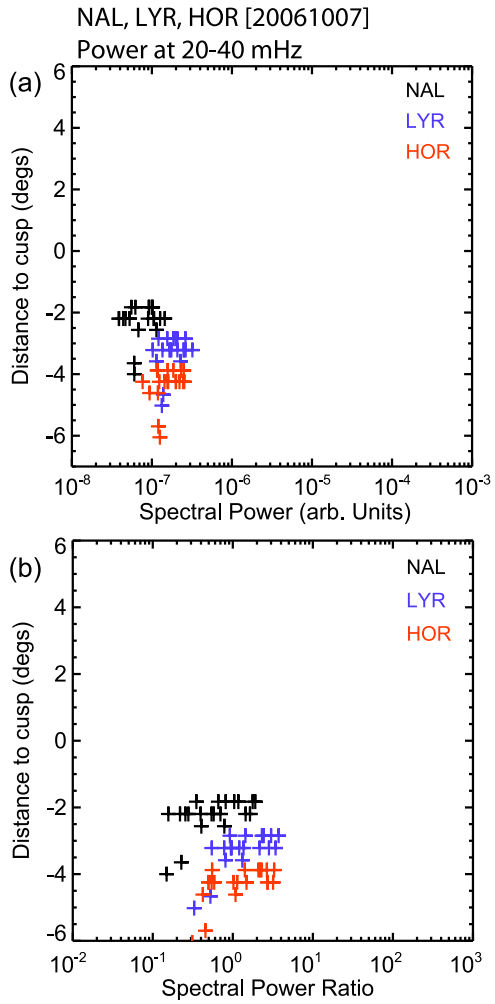

Figure 7. (a) A scatterplot of the NAL, LYR and HOR magnetometer spectral power as displayed in Figure 6b against the latitudinal separation of the magnetometer station from the spectral width cusp proxy indicated in Figure 6a. (b) As for Figure 7a but now plotting the magnetometer spectral power normalized by the concurrent spectral power measured by HAL.

magnetometer latitude separations of 6° or more, with a further 7 days showing 4° or more. The separation of the latitude of maximum Pc3 power from the cusp latitude on a particular day varied between 4° equatorward of the cusp to 0.5° poleward on one occasion. Half of the days had sufficient variability of the cusp location to individually show a clear trend in Pc3 power with separation from the cusp. While a great deal of scatter is apparent in Figure 8a, a clear overall peak in spectral power is observed close to 2° equatorward of the cusp location. Figure 8b presents the same data, but with the color-coding removed for clarity, and the mean spectral power in 1° latitude bins overplotted, together with the standard errors on the mean powers. 1° latitude bins are chosen as, although magnetometer data responds to a region integrated over approximately the E region height, somewhat greater than 1°, the overhead currents will provide the strongest signatures, and clear variations in power are observed between the Svalbard magnetometers at separations of ~1°. In spite of the scatter in the plot, the mean powers can be seen to be well ordered by their proximity to the cusp. Figure 9 presents a similar analysis for the spectral power ratio. The peak power at 2° equatorward of the cusp location is retained in this figure, and the spread of the data remains similar to that shown in Figure 8.

4. Discussion

[20] Data from 14 intervals of induction coil magnetometer measurements from a closely spaced array on Svalbard have been combined with data from the Hankasalmi SuperDARN radar to investigate the dependence of Pc3 wave power in the ground based magnetometer data, originating from upstream of the bow shock, on the proximity of the magnetometers to the cusp region. Wave power has been quantified by summing the spectral power in the magnetometer data between 20 and 40 mHz, using both the spectral power measured in the vicinity of the cusp, and the ratio of spectral powers in the cusp region to that measured deeper in the magnetosphere at HAL. The latitudinal separation of the magnetometers from the cusp region was monitored by the location of the spectral width boundary in the ionospheric backscatter from the Hankasalmi radar, which has been shown here to be an effective diagnostic of the cusp location for use with the the Augsburg College–University of New Hampshire magnetometer array on Svalbard. Pc3 ULF wave activity has been demonstrated to be modulated as the open-closed field line boundary, as predicted from the Hankasalmi radar data, migrates across the magnetometer array. Both radar and magnetometer measurements have been processed at a cadence of 5 min, leading to a total of 1364 data points being available for comparison.

[21] Two intervals have been examined in detail. Figure 4 presented the cusp location and integrated Pc3 spectral power from one of the longer intervals of data on February 21, 2008. This extended interval allows the variability of the Pc3 spectral power to be examined as the cusp latitude changes significantly. From 06:30 UT to 10:00 UT the cusp remained significantly poleward of the magnetometer stations, and the spectral power from the highest latitude magnetometer at NAL is consistently lower than that recorded at the two lower latitude stations, indicating that on this day the latitude of the peak spectral power was significantly displaced equatorward of the cusp position. Early in the interval LYR records higher powers than the lower latitude HOR station, indicating that the equatorward displacement of the maximum Pc3 spectral power location from the cusp is modest. By 11:00 UT it was the HOR station which recorded the highest spectral powers, indicating that as the cusp location moved equatorward, the location of the peak Pc3 spectral power migrated equatorward in concert with the cusp location, but now to latitudes equatorward of all three magnetometer stations. By the end of the interval, when the cusp itself had migrated equatorward of the magnetometer stations, the spectral power was clearly ordered, decreasing with latitude, indicating a drop off in Pc3 spectral power as the poleward latitude separation of the magnetometers from the cusp increased.

[22] The scatterplot of integrated Pc3 spectral power versus separation from the cusp presented in Figure 5 confirms this behavior, showing a strong ordering of the Pc3 spectral

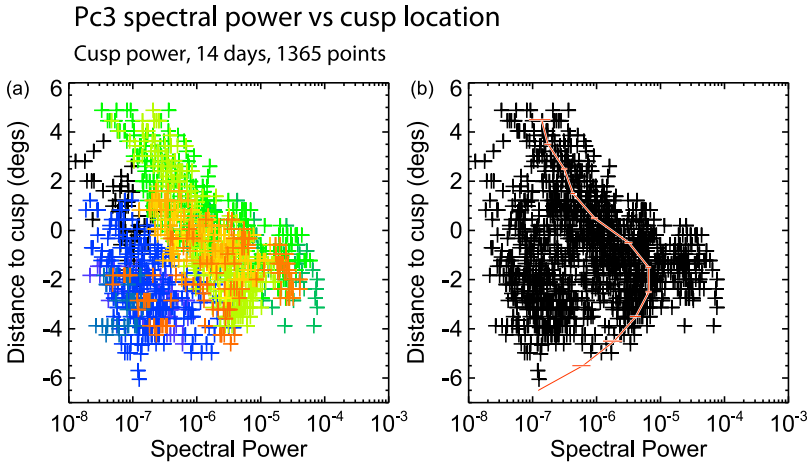

Figure 8. A scatterplot of the NAL, LYR and HOR magnetometer spectral power for each station against the latitudinal separation of the magnetometer station from the cusp, as displayed in Figures 5 and 7, but now for the full ensemble of 14 days data. In Figure 8a the data are color-coded according to the day on which the observations were taken, in order to highlight the trends during and between days. In Figure 8b the color-coding is removed, and the mean power and standard error on the mean power in 1° latitude bins is overplotted on the raw data.

power with cusp separation, with the displacement of the spectral power peak from the cusp being ~2° equatorward. A consistent pattern is displayed for each of the Svalbard magnetometers. Very similar behavior was observed in the spectral powers from the Svalbard stations when presented as a spectral power and a spectral power ratio normalized by the spectral power recorded at the lower latitude station at Halley, indicating that any temporal variability of the upstream source was not a strong or significant influence on the latitudinal dependence of spectral power shown in Figure 5a.

[23] A similar picture emerges from the second interval on October 7, 2006 examined in Figure 6. This shorter interval has less variability in the cusp location, which remains poleward of all three magnetometer stations throughout. However, the data from the Hankasalmi radar clearly indicate that the cusp latitude was at its lowest during the central hour of the interval. The highest latitude station at NAL recorded the lowest integrated Pc3 spectral powers throughout, again indicating that the location of the peak power was displaced equatorward of the cusp. Pc3 power at the middle latitude station at LYR dominated at the beginning and the end of the interval when the cusp latitude was highest, whereas the lowest latitude station at HOR was strongest in the middle of the interval when the cusp was at its lowest latitude. The scatterplot for this interval (Figure 7) showed much less variability in the recorded spectral power, as might be expected for a more constant cusp position, and in this case there is some evidence for the peak spectral power lying some 4° equatorward of the cusp position. Again the data from the three Svalbard stations are consistent, and a similar picture emerges from the spectral power and spectral power ratio analysis.

[24] The full data ensemble were presented in Figure 8. When combined together the 14 days data present a much

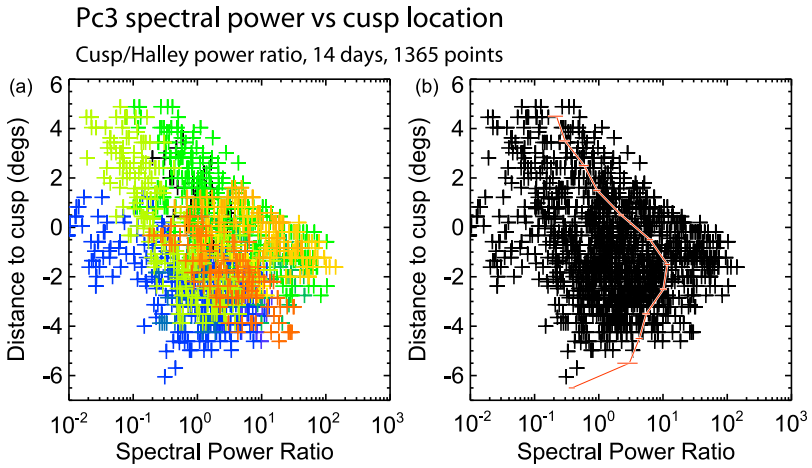

Figure 9. A scatterplot of the NAL, LYR and HOR magnetometer spectral power, normalized by the concurrent spectral power measured by HAL, for each station against the latitudinal separation of the magnetometer station from the cusp, in the same format as Figure 8.

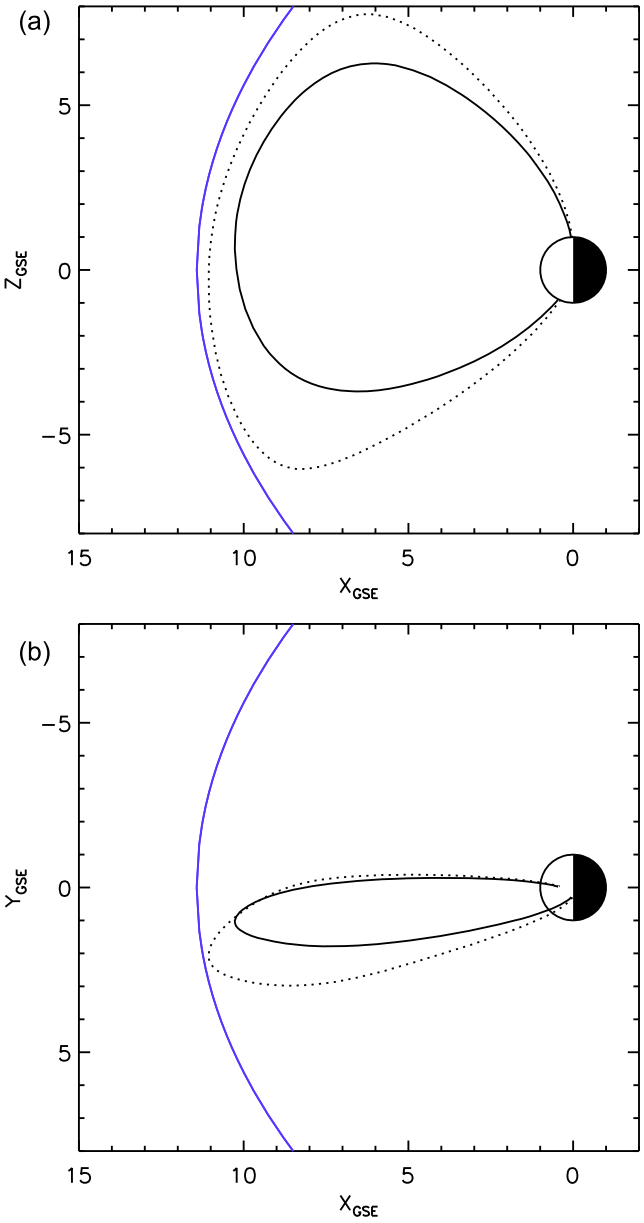

Figure 10. A Tsyganenko 96 field line trace of the last closed field line (dotted line), and the field line corresponding to the latitude of the peak Pc3 spectral power observations in the vicinity of the cusp (solid line). (a) GSE XZ plane and (b) GSE XY plane. A model magnetopause is indicated in blue in each panel.

more scattered picture than when examined individually. The color-coding by day of observation in Figure 8a reveals that while individual days are well ordered by the location relative to the cusp, there are significant differences in power level between the various days of observations, with, for example the observations color-coded blue showing greatly reduced Pc3 wave power compared to the day color coded green. This is perhaps unsurprising, as differing intensities of the upstream wave source and differing efficiencies of wave propagation through the magnetosheath and magnetosphere to the cusp footprint region are to be expected on different days, with different magnetospheric conditions. In spite of this spread in the data, when the mean Pc3 spectral power is calculated in 1° latitude bins in Figure 8b, a clear trend for maximum power at ~2° latitude equatorward of the cusp location remains, in spite of the actual spectral power recorded at this location varying by ~ three orders of magnitude between individual observations taken in this region. The standard deviation of the distribution at the peak ~2° equatorward of the cusp is large at $\sim 10^{-5}$ arbitrary units compared to the mean of $\sim 6 \times 10^{-6}$. However the standard error on the mean powers plotted in Figure 8b remain of modest size at $\sim 7 \times 10^{-7}$. A linear fit to the mean powers poleward and equatorward of the peak give power gradients corresponding to an order of magnitude power decrease in 3.3° latitude poleward of the maximum and 2.2° latitude equatorward of the maximum.

[25] The full data ensemble in terms of spectral power ratios between the Svalbard stations and the lower latitude station at Halley were presented in Figure 9. This figure presents a very similar picture to Figure 8. Again there is a large spread in the data from day to day, with spectral power ratios ranging from 10^{-2} to 10^{2}, but a clear tendency for the peak spectral power ratio to be recorded in a region ~2° equatorward of the cusp location remains. A linear fit to the mean powers ratios poleward and equatorward of the peak give power ratio gradients corresponding to an order of magnitude power ratio decrease in 3.2° latitude poleward of the maximum and between 2.6 and 5.6° latitude equatorward of the maximum, depending on whether or not the lowest latitude mean datapoint is used in the fit. At the lowest latitudes the data are sparse and a linear fit is probably not appropriate for the spectral power ratio data. Thus we conclude there is no detectable difference in the latitudinal gradients for the spectral power and spectral power ratio results in the current analysis.

[26] Figure 9 shows that the Pc3 spectral power is typically amplified by a factor of ~10 in the region of maximum power equatorward of the cusp when compared to the lower latitude data from Halley at $L = 4.6$. The standard deviation of the distribution at the peak ~2° equatorward of the cusp is ~20, with the standard error on the mean of ~1. The spectral power in the high latitude region falls off away from the location of the peak spectral power such that it typically equals that at Halley (a spectral power ratio of 1) at ~3° poleward of the spectral power peak, and again between 2.6° and 5.6° equatorward of the spectral power peak. Hence spectral power at the cusp latitude itself is broadly the same as that observed in the inner magnetosphere. At times the spectral power far from the cusp at HAL may exceed that at the cusp by up to an order of magnitude, indicating that wave entry to the inner magnetosphere may be stronger than that to the cusp region. During the intervals examined here the high latitude (northern hemisphere) stations are predominantly under winter conditions, whereas the lower latitude (southern hemisphere) station is under summer conditions. The seasonal variation of, for example, ionospheric conductivity will likely have an effect on the measured Pc3 powers and hence the spectral power ratios, and this will be investigated in future studies.

[27] It is interesting to estimate the location within the equatorial plane magnetosphere which corresponds to the region of maximum Pc3 spectral power on the ground. To do this Figure 10 presents a field line trace using the

Tsyganenko 96 (T96 [*Tsyganenko*, 1995]) geomagnetic field model, driven by upstream parameters appropriate for the interval of February 21, 2008, (which was presented in Figures 3–5) at 10:00 UT. This interval is typical for the intervals under investigation here. Figure 10a shows the GSE XZ plane and Figure 10b shows the GSE XY plane, and a model magnetopause [*Shue et al.*, 1997] is indicated in each panel for reference. The dotted line represents a field line which reaches the magnetopause. The solid line represents a field line emanating from a location 2° equatorward of this, typical of the region of maximum Pc3 wave power for the data examined here. The peak Pc3 wave power can be seen to correspond to a location ~1 Earth radius (R_E) inside the magnetopause.

[28] The location of the Pc3 spectral power maximum presented here, some 2° equatorward of the cusp location, and 1 R_E inside the equatorial magnetopause, argues against the mechanism involving a waveguide in the exterior cusp presented by *Pilipenko et al.* [1999]. As outlined in section 1 and by *Howard and Menk* [2005], the direct propagation of a fast mode wave and a cavity mode mechanism also appear not to match these or previous observations. However, the location of the observed peak wave power does map to closed field lines in the outer magnetosphere close to the equatorward boundary of the cusp, as proposed in the ionospheric transistor mechanism originally introduced by *Engebretson et al.* [1991a], and further reviewed by *Engebretson et al.* [2006].

[29] Comparing the latitude profile of Pc3 power here with that investigated by *Howard and Menk* [2005], the Svalbard stations used here lie at the latitudes which typically measured the maximum Pc3 power in that study, whereas HAL lies toward the lower end of their latitude range, where typically much lower Pc3 powers were recorded. The observations presented here are also consistent with the profiles presented in Figure 10 of *Howard and Menk* [2005] for a partially coupled fast mode, where the fast mode couples to a field guided Alfvén mode, which transmits the wave energy to the ionosphere as a traveling wave, rather than a strongly coupled FLR which would result in a clear standing wave on a field line. According to this study such a scenario could also lead to a peak in Pc3 power 2–3° equatorward of a modeled magnetopause footprint, although the well-defined region of enhanced Pc3 power appears more consistent with the ionospheric transistor mechanism. Here we have supplemented the studies described by *Engebretson et al.* [2006] and that of *Howard and Menk* [2005] by providing an improved experimental measurement of the cusp location. We have also included all Pc3 power, rather than restrict the study to events with a large spatial coherence length as in the work of *Howard and Menk* [2005], albeit with a limited data set of 14 days.

[30] The spread of the measured Pc3 wave power in the cusp region presented in Figure 8 is very similar to that in the Pc3 wave power normalized by the wave power at Halley in Figure 9. Thus it appears that the spatial structure of the wave power deeper within the magnetosphere, presumably arising due the wave power effectively entering the inner magnetosphere where it can couple to Alfvén modes as described by *Howard and Menk* [2005], and *Clausen et al.* [2008, 2009], seems to be as important in contributing to the spread in the distribution of the wave power as the temporal variability in the upstream wave source, and indeed imposes a similar magnitude of control over the wave power as the proximity to the cusp. While the Pc3 wave power is known to penetrate into the low latitude region, as described by *Yumoto et al.* [1984, 1985], where the local field line resonant frequencies match the Pc3 wave source, this suggests that significant wave coupling can also occur at the mid geomagnetic latitudes occupied by HAL, a region which lies equatorward of the main Pc3 power peak recorded by *Engebretson et al.* [1991a], *Howard and Menk* [2005] and also recorded in this study. *Clausen et al.* [2008] demonstrated that the time of arrival of wave activity over a wide range of ground magnetometer stations was consistent with the propagation of the wave power from the subsolar magnetopause, and also presented evidence of the coupling of this wave power to local field line resonances at mid latitudes. This was confirmed by Cluster observations in the work of *Clausen et al.* [2009]. The proximity of a midlatitude station such as HAL to such a coupling region would clearly have a significant influence on the normalized Pc3 power such as is displayed in Figure 9.

5. Conclusions

[31] Induction coil magnetometer measurements from a closely spaced array on Svalbard have been combined with measurements of the location of the cusp derived from the spectral width boundary data from the Hankasalmi SuperDARN radar to investigate the dependence of Pc3 wave power in the ground based magnetometer data, originating from upstream of the bow shock, on the proximity of the magnetometers to the cusp region. The data have revealed that a robust maximum of Pc3 spectral power exists centered on a region 2° equatorward of the cusp location. Taken with previous studies of the spatial distribution of Pc3 power the experimental evidence of high wave powers near the cusp argues against the direct entry of fast mode wave power to the magnetosphere or a cavity mode mechanism. The equatorward displacement of the Pc3 power peak also argues against wave transmission through a waveguide in the exterior cusp or through modulation of the cusp currents. The cusp region data are consistent with the ionospheric transistor model of *Engebretson et al.* [1991a]. A partially coupled fast mode, where the fast mode couples to a field guided Alfvén mode, which transmits the wave energy to the ionosphere as a traveling wave also offers a possible alternative mechanism for producing the data, and probably contributes strongly to the scatter of data observed in Figure 9, strongly influencing the global distribution of Pc3 power. However the ionospheric transistor mechanism appears to provide a robust explanation for the well-defined region of enhanced Pc3 power in the cusp region.

[32] The spatial structure of the wave power within the magnetosphere, presumably arising due the wave power effectively entering the inner magnetosphere where it can couple to Alfvén modes as described by *Howard and Menk* [2005], seems to be as important in contributing to the spread in the distribution of the wave power as the temporal variability in the upstream wave source.

[33] **Acknowledgments.** The work by T.K.Y. is supported by STFC grant ST/H002480/1. The Hankasalmi SuperDARN radar operations were funded by STFC grant PP/E007929/1. The search coil magnetometer array on Svalbard was supported by U.S. National Science Foundation grants ARC-0806196 to Augsburg College and ARC-0806338 to the University of New Hampshire. The DMSP particle detectors were designed by Dave Hardy of AFRL, and data obtained from JHU/APL.

[34] Robert Lysak thanks the reviewers for their assistance in evaluating this paper.

References

Baker, K. B., J. R. Dudeney, R. A. Greenwald, M. Pinnock, P. T. Newell, A. S. Rodger, N. Mattin, and C. I. Meng (1995), HF radar signatures of the cusp and low-latitude boundary layer, *J. Geophys. Res.*, *100*, 7671–7695, doi:10.1029/94JA01481.

Chisham, G., and M. P. Freeman (2003), A technique for accurately determining the cusp-region polar cap boundary using superdarn HF radar measurements, *Ann. Geophys.*, *21*, 983–996, doi:10.5194/angeo-21-983-2003.

Chisham, G., et al. (2007), A decade of the Super Dual Auroral Radar Network (SuperDARN): Scientific achievements, new techniques and future directions, *Surv. Geophys.*, *28*, 33–109, doi:10.1007/s10712-007-9017-8.

Chisham, G., T. Yeoman, and G. J. Sofko (2008), Mapping ionospheric backscatter measured by the SuperDARN HF radars - part 1: A new empirical virtual height model, *Ann. Geophys.*, *26*, 823–841, doi:10.5194/angeo-26-823-2008.

Clausen, L. B. N., T. K. Yeoman, R. Behlke, and E. A. Lucek (2008), Multi-instrument observations of a large scale Pc4 pulsation, *Ann. Geophys.*, *26*, 185–199, doi:10.5194/angeo-26-185-2008.

Clausen, L. B. N., T. K. Yeoman, R. C. Fear, R. Behlke, E. A. Lucek, and M. J. Engebretson (2009), First simultaneous measurements of waves generated at the bow shock in the solar wind, the magnetosphere and on the ground, *Ann. Geophys.*, *27*, 357–371, doi:10.5194/angeo-27-357-2009.

Engebretson, M. J., L. J. Cahill, R. L. Arnoldy, B. J. Anderson, T. J. Rosenberg, D. L. Carpenter, U. S. Inan, and R. H. Eather (1991a), The role of the ionosphere in coupling upstream ULF wave power into the dayside magnetosphere, *J. Geophys. Res.*, *96*, 1527–1542, doi:10.1029/90JA01767.

Engebretson, M. J., N. Lin, W. Baumjohann, H. Lühr, B. J. Anderson, L. J. Zanetti, T. A. Potemra, R. L. McPherron, and M. G. Kivelson (1991b), A comparison of ULF fluctuations in the solar wind, magnetosheath, and dayside magnetosphere: 1. Magnetosheath morphology, *J. Geophys. Res.*, *96*, 3441–3454, doi:10.1029/90JA02101.

Engebretson, M. J., J. R. Beck, R. L. Rairden, S. B. Mende, R. L. Arnoldy, L. J. Cahill Jr., and T. J. Rosenberg (1994a), Studies of the occurrence and properties of Pc 3–4 magnetic and auroral pulsations at south pole, Antarctica, in *Solar Wind Sources of Magnetospheric Ultra-Low-Frequency Waves*, *Geophys. Monogr. Ser.*, vol. 81, edited by M. J. Engebretson, K. Takahashi, and M. Scholer, pp. 345–353, AGU, Washington, D. C.

Engebretson, M. J., J. R. Beck, T. J. Rosenberg, R. L. Rairden, S. B. Mende, R. L. Arnoldy, and L. J. Cahill Jr. (1994b), Optical evidence that modulated electron precipitation near the magnetospheric boundary drives high latitude Pc 3–4 magnetic pulsations, in *Physical Signatures of Magnetospheric Boundary Layer Processes*, edited by J. A. Holtet and A. Egeland, *NATO ASI Ser., Ser. C*, *425*, 361–373.

Engebretson, M. J., R. K. Cobian, J. L. Posch, and R. L. Arnoldy (2000), A conjugate study of Pc3-4 pulsations at cusp latitudes: Is there a clock angle effect?, *J. Geophys. Res.*, *105*, 15,965–15,980, doi:10.1029/1999JA000328.

Engebretson, M. J., et al. (2005), On the source of Pc 1–2 waves in the plasma mantle, *J. Geophys. Res.*, *110*, A06201, doi:10.1029/2004JA010515.

Engebretson, M. J., J. L. Posch, V. Pilipenko, and O. Chugunova (2006), ULF waves at very high latitudes, in *Magnetospheric ULF Waves: Synthesis and New Directions*, *Geophys. Monogr. Ser.*, vol. 169, edited by K. Takahashi et al., pp. 137–156, AGU, Washington, D. C.

Engebretson, M. J., J. Moen, J. L. Posch, F. Lu, M. R. Lessard, H. Kim, and D. A. Lorentzen (2009), Searching for ULF signatures of the cusp: Observations from search coil magnetometers and auroral imagers in Svalbard, *J. Geophys. Res.*, *114*, A06217, doi:10.1029/2009JA014278.

Gary, S. P. (1981), Microinstabilities upstream of the Earth's bow shock: A brief review, *J. Geophys. Res.*, *86*, 4331–4336, doi:10.1029/JA086iA06p04331.

Greenstadt, E. W., R. L. McPherron, and K. Takahashi (1981), Solar wind control of daytime, midperiod geomagnetic pulsations, in *ULF Pulsations in the Magnetosphere*, pp. 89–110, D. Reidel, Dordrecht, Netherlands.

Greenwald, R. A., et al. (1995), DARN/SuperDARN a global view of the dynamics of high-latitude convection, *Space Sci. Rev.*, *71*, 761–796, doi:10.1007/BF00751350.

Hardy, D. A., L. K. Schmitt, M. S. Gussenhoven, F. J. Marshall, H. C. Yeh, T. L. Shumaker, A. Hube, and J. Pantazis (1984), Precipitating electron and ion detectors (SSJ/4) for the block 5D/Flights 6–10 DMSP satellites: Calibration and data presentation, *Rep. AFGL-TR-84-0317*, Air Force Geophys. Lab., Hanscom Air Force Base, Mass.

Howard, T. A., and F. W. Menk (2005), Ground observations of high-latitude Pc3-4 ULF waves, *J. Geophys. Res.*, *110*, A04205, doi:10.1029/2004JA010417.

Kivelson, M. G., J. Etcheto, and J. G. Trotignon (1984), Global compressional oscillations of the terrestrial magnetosphere: the evidence and a model, *J. Geophys. Res.*, *89*, 9851–9856, doi:10.1029/JA089iA11p09851.

Krauss-Varban, D. (1994), Bow shock and magnetosheath simulations: Wave transport and kinetic properties, in *Solar Wind Sources of Magnetospheric Ultra-Low-Frequency Waves*, edited by M. J. Engebretson, K. Takahashi, and M. Scholer, pp. 121–134, AGU, Washington D. C.

Lester, M., et al. (2004), Stereo CUTLASS—A new capability for the SuperDARN HF radars, *Ann. Geophys.*, *22*, 459–473, doi:10.5194/angeo-22-459-2004.

Lin, N., M. J. Engebretson, R. L. McPherron, M. G. Kivelson, W. Baumjohann, H. Lühr, T. A. Potemra, B. J. Anderson, and L. J. Zanetti (1991a), A comparison of ULF fluctuations in the solar wind, magnetosheath, and dayside magnetosphere: 2. Field and plasma conditions in the magnetosheath, *J. Geophys. Res.*, *96*, 3455–3464, doi:10.1029/90JA02098.

Lin, N., M. J. Engebretson, W. Baumjohann, and H. Lühr (1991b), Propagation of perturbation energy fluxes in the subsolar magnetosheath, AMPTE IRM observations, *Geophys. Res. Lett.*, *18*, 1667–1670, doi:10.1029/91GL01849.

Matsuoka, H., A. S. Yukimatu, H. Yamagishi, N. Sato, G. J. Sofko, B. J. Fraser, P. Ponomarenko, R. Liu, and T. Goka (2002), Coordinated observations of Pc3 pulsations near cusp latitudes, *J. Geophys. Res.*, *107*(A11), 1400, doi:10.1029/2001JA000065.

McWilliams, K. A., T. K. Yeoman, and S. W. H. Cowley (2001), Two-dimensional electric field measurements in the ionospheric footprint of a flux transfer event, *Ann. Geophys.*, *18*, 1584–1598, doi:10.1007/s00585-001-1584-2.

Newell, P. T., and C. I. Meng (1992), Mapping the dayside ionosphere to the magnetosphere according to particle precipitation characteristics, *Geophys. Res. Lett.*, *19*, 609–612, doi:10.1029/92GL00404.

Odera, T. J. (1986), Solar wind controlled pulsations: A review, *Rev. Geophys.*, *24*, 55–74.

Pilipenko, V., and M. Engebretson (2002), Ground images at high latitudes of ULF wave processes in the outer magnetosphere, *J. Atmos. Sol. Terr. Phys.*, *64*, 183–201, doi:10.1016/S1364-6826(01)00083-9.

Pilipenko, V., E. Fedorov, N. Mazur, M. J. Engebretson, and W. J. Hughes (1999), Magnetohydrodynamic waveguide/resonator for Pc 3 ULF waves at cusp latitudes, *Earth Planets Space*, *51*, 441–448.

Ponomarenko, P. V., C. L. Waters, and F. W. Menk (2007), Factors determining spectral width of HF echoes from high latitudes, *Ann. Geophys.*, *25*, 675–687, doi:10.5194/angeo-25-675-2007.

Ruohoniemi, J. M., and R. A. Greenwald (1996), Statistical patterns of high-latitude convection obtained from goose bay HF radar observations, *J. Geophys. Res.*, *101*, 21,743–21,764, doi:10.1029/96JA01584.

Ruohoniemi, J. M., and R. A. Greenwald (2005), Dependencies of high-latitude plasma convection: Consideration of interplanetary magnetic field, seasonal, and universal time factors in statistical patterns, *J. Geophys. Res.*, *110*, A09204, doi:10.1029/2004JA010815.

Shue, J.-H., J. K. Chao, H. C. Fu, C. T. Russell, P. Song, K. K. Khurana, and H. J. Singer (1997), A new functional form to study the solar wind control of the magnetopause size and shape, *J. Geophys. Res.*, *102*, 9497, doi:10.1029/97JA00196.

Southwood, D. J. (1974), Some features of field line resonances in the magnetosphere, *Planet Space Sci.*, *22*, 483–491, doi:10.1016/0032-0633(74)90078-6.

Takahashi, K., R. L. McPherron, and T. Terasawa (1984), Dependence of the spectrum of Pc 3–4 pulsations on the interplanetary magnetic field, *J. Geophys. Res.*, *89*, 2770–2780, doi:10.1029/JA089iA05p02770.

Troitskaya, V. A., T. A. Plyasova-Bakunina, and A. V. Gul'elmi (1971), Relationship between Pc 2–4 pulsations and the interplanetary field, *Dokl. Akad. Nauk SSSR*, *197*, 1312–1314.

Tsyganenko, N. A. (1995), Modeling the Earth's magnetospheric magnetic field confined within a realistic magnetopause, *J. Geophys. Res.*, *100*, 5599–5612, doi:10.1029/94JA03193.

Villain, J. P., R. André, M. Pinnock, R. A. Greenwald, and C. Hanuise (2002), A statistical study of the Doppler spectral width of high-latitude ionospheric F-region echoes recorded with SuperDARN coherent HF radars, *Ann. Geophys.*, *20*, 1769–1781, doi:10.5194/angeo-20-1769-2002.

Yeoman, T. K., D. M. Wright, A. J. Stocker, and T. B. Jones (2001), An evaluation of range accuracy in the SuperDARN over-the-horizon HF radar systems, *Radio Sci.*, *36*, 801–813, doi:10.1029/2000RS002558.

Yeoman, T. K., G. Chisham, L. J. Baddeley, R. S. Dhillon, T. J. T. Karhunen, T. R. Robinson, A. Senior, and D. M. Wright (2008), Mapping ionospheric backscatter measured by the superdarn HF radars - part 2: Assessing SuperDARN virtual height models, *Ann. Geophys.*, *26*, 843–852, doi:10.5194/angeo-26-843-2008.

Yumoto, K., T. Saito, B. T. Tsurutani, E. J. Smith, and S.-I. Akasofu (1984), Relationship between the IMF magnitude and Pc3 magnetic pulsations in the magnetosphere, *J. Geophys. Res.*, *89*, 9731–9740, doi:10.1029/JA089iA11p09731.

Yumoto, K., T. Saito, S.-I. Akasofu, B. T. Tsurutani, and E. J. Smith (1985), Propagation mechanism of daytime Pc3-4 pulsation observed at synchronous orbit and multiple ground-based stations, *J. Geophys. Res.*, *90*, 6439–6450, doi:10.1029/JA090iA07p06439.

M. J. Engebretson, Department of Physics, Augsburg College, Minneapolis, MN 55454, USA.

H. Kim, Center for Space Science and Engineering Research, Virginia Polytechnic Institute and State University, Blacksburg, VA 24061, USA.

M. R. Lessard, Space Science Center, University of New Hampshire, Durham, NH 03824, USA.

V. A. Pilipenko, Space Research Institute, 117997 Moscow, Russia.

D. M. Wright and T. K. Yeoman, Department of Physics and Astronomy, University of Leicester, Leicester LE1 7RH, UK. (tim.yeoman@ion.le.ac.uk)